1-1-2008

Simultaneous multiwavelength observations of magnetic activity in ultracool dwarfs. I. The complex behavior of the M8.5 dwarf TVLM 513-46546

E. Berger

J. E. Gizis

M. S. Giampapa

R. E. Rutledge

J. Liebert

See next page for additional authors

The Astrophysical Journal, 673:1080–1087, 2008 February 1

SIMULTANEOUS MULTIWAVELENGTH OBSERVATIONS OF MAGNETIC ACTIVITY IN ULTRACOOL DWARFS. I. THE COMPLEX BEHAVIOR OF THE M8.5 DWARF TVLM 513−46546

E. Berger,[1,2,3] J. E. Gizis,[4] M. S. Giampapa,[5] R. E. Rutledge,[6] J. Liebert,[7] E. Martín,[8,9] G. Basri,[10] T. A. Fleming,[7] C. M. Johns-Krull,[11] N. Phan-Bao,[9] and W. H. Sherry[5]

Received 2007 August 10; accepted 2007 October 19

ABSTRACT

We present the first simultaneous radio, X-ray, ultraviolet, and optical spectroscopic observations of the M8.5 dwarf TVLM 513−46546, with a duration of 9 hr. These observations are part of a program to study the origin of magnetic activity in ultracool dwarfs, and its impact on chromospheric and coronal emission. Here we detect steady quiescent radio emission superposed with multiple short-duration, highly polarized flares; there is no evidence for periodic bursts previously reported for this object, indicating their transient nature. We also detect soft X-ray emission, with $L_X/L_{bol} \approx 10^{-5.1}$, the faintest to date for any object later than M5, and a possible X-ray flare. TVLM 513−46546 continues the trend of severe violation of the radio/X-ray correlation in ultracool dwarfs, by nearly 4 orders of magnitude. From the optical spectroscopy we find that the Balmer line luminosity exceeds the X-ray luminosity by a factor of a few, ruling out chromospheric heating by coronal X-ray emission. More importantly, we detect sinusoidal Hα and Hβ equivalent width light curves with a period of 2 hr, matching the rotation period of TVLM 513−46546. This behavior points to a corotating chromospheric hot spot or an extended magnetic structure, with a covering fraction of about 50%. This feature may be transitory based on the apparent decline in light-curve peak during the four observed maxima. From the radio data we infer a large-scale and steady magnetic field of $\sim 10^2$ G. A large-scale field is also required by the sinusoidal Balmer line emission. The radio flares, on the other hand, are produced in a component of the field with a strength of $\sim$3 kG and a likely multipolar configuration. The overall lack of correlation between the various activity indicators suggests that the short-duration radio flares do not have a strong influence on the chromosphere and corona, and that the chromospheric emission is not the result of coronal heating.

Subject headings: radio continuum: stars — stars: activity — stars: low-mass, brown dwarfs — stars: magnetic fields

1. INTRODUCTION

In recent years it has become evident that low-mass stars and brown dwarfs (spectral classes late-M and L) are capable of producing unanticipated levels of magnetic activity, manifested primarily in their strong quiescent and flaring radio emission (Berger et al. 2001, 2005; Berger 2002, 2006; Burgasser & Putman 2005; Osten et al. 2006; Antonova et al. 2007; Phan-Bao et al. 2007; Hallinan et al. 2007; Audard et al. 2007). Other traditional activity indicators such as chromospheric Balmer line emission and coronal X-ray emission, however, appear to steeply decline from peak levels in early- and mid-M dwarfs (Pallavicini et al. 1981; Vilhu & Walter 1987; Gizis et al. 2000; West et al. 2004), leading to divergent trends of magnetic activity at the bottom of the main sequence. In both Hα and X-rays there is also a clear transition from persistent emission to a small number of flaring objects with duty cycles of a few percent (Reid et al. 1999; Gizis et al. 2000; Rutledge et al. 2000; Liebert et al. 2003; West et al. 2004), as well as a breakdown of the rotation-activity relation (Basri & Marcy 1995; Mohanty & Basri 2003) that is clearly seen in early M dwarfs (Rosner et al. 1985; Fleming et al. 1993; Mohanty et al. 2002; Pizzolato et al. 2003).

The change and divergence in activity trends is most clearly evident in the breakdown of the radio/X-ray correlation that holds for a large number of early-type stars and solar flares (Güdel & Benz 1993; Güdel et al. 1993a; Benz & Güdel 1994), and is attributed to flare heating of coronal plasma to X-ray temperatures (Neupert 1968; Güdel et al. 1996). While objects in the range M0–M6 obey this correlation, several objects later than M7 exhibit radio emission that is several orders of magnitude brighter than expected (Berger et al. 2001, 2005; Berger 2002, 2006). Similarly, in early M dwarfs there is an overall energy balance between X-ray and chromospheric emission, which has led to the idea of chromospheric heating by coronal X-rays (e.g., Cram 1982; Hawley et al. 1995). It is not known whether this mechanism holds in ultracool dwarfs, primarily because of the decline in persistent activity.

Theoretical work on magnetic dynamos in ultracool dwarfs also remains inconclusive. Studies of the α^2 dynamo in fully convective stars suggest that a stratified and rotating turbulent medium can lead to the buildup of a nonaxisymmetric and multipolar field (e.g., Chabrier & Küker 2006; Dobler et al. 2006), but these models make several simplifications for computational purposes. It has also been argued that decreasing electrical conductivity will

[1] Observatories of the Carnegie Institution of Washington, 813 Santa Barbara Street, Pasadena, CA 91101.
[2] Princeton University Observatory, Peyton Hall, Ivy Lane, Princeton, NJ 08544.
[3] Hubble Fellow.
[4] Department of Physics and Astronomy, University of Delaware, Newark, DE 19716.
[5] National Solar Observatory, National Optical Astronomy Observatories, Tucson, AZ 85726.
[6] Department of Physics, McGill University, Rutherford Physics Building, 3600 University Street, Montreal, QC H3A 2T8, Canada.
[7] Department of Astronomy and Steward Observatory, University of Arizona, 933 North Cherry Avenue, Tucson, AZ 85721.
[8] Instituto de Astrofísica de Canarias, C/Vía Láctea s/n, E-38200 La Laguna, Tenerife, Spain.
[9] University of Central Florida, Department of Physics, P.O. Box 162385, Orlando, FL 32816.
[10] Astronomy Department, University of California, Berkeley, CA 94720.
[11] Department of Physics and Astronomy, Rice University, 6100 Main Street, MS-61, Houston, TX 77005.

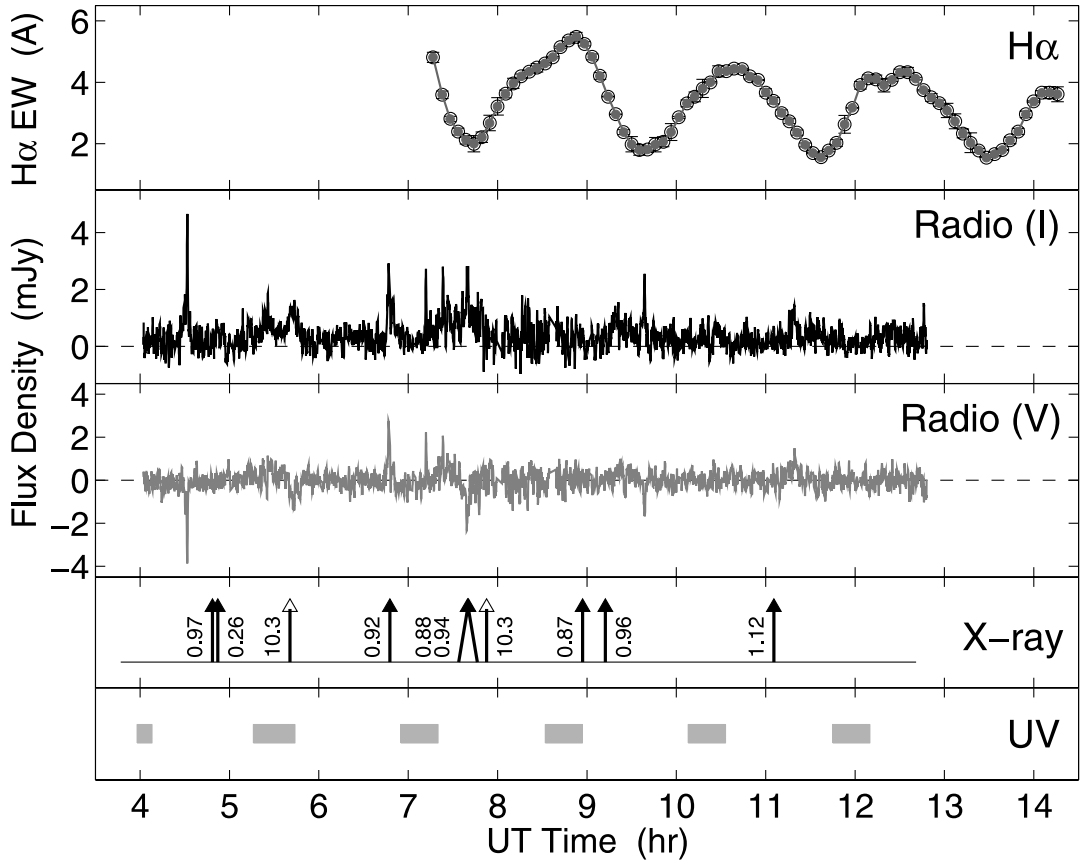

FIG. 1.—Radio, Hα, UV, and X-ray of TVLM 513−46546. The arrival times of the X-ray photons are shown with arrows, and their energies in keV are listed. Open arrows correspond to likely background events with ∼10 keV; two are expected from the background count rate. Times of UV coverage are marked by squares; no UV emission is detected. The Hα emission is clearly sinusoidal and periodic, with $P \approx 2$ hr matching the rotation period of TVLM 513−46546, with an implied $\sin i \approx 1$. There is no clear correspondence between the various emission bands, with the possible exception of an X-ray photon pair that coincides with the broadest radio flare (at about 07:40 UT).

impede the dissipation of any magnetic fields in the cool and increasingly neutral atmospheres of ultracool dwarfs (Mohanty et al. 2002). The existing radio detections suggest that field dissipation may not be a problem, but the overall field configuration and the effect of neutral atmospheres in the presence of magnetic dissipation remain largely unexplored.

As a result of the various conflicting trends and the transition from persistent to flaring emission, progress in our understanding of magnetic activity and dynamos in ultracool dwarfs requires *simultaneous* observations of the various activity bands. We have already undertaken such observations for the L3.5 brown dwarf 2MASS J00361617+1821104 in late 2002 and discovered periodic radio emission ($P = 184$ minutes), with no corresponding X-ray or Hα emission (Berger et al. 2005). These observations indicated a magnetic field of ∼200 G covering a substantial fraction of the stellar surface, as well as the first direct confirmation that the radio/X-ray correlation is indeed violated by orders of magnitude. Follow-up observations showed that the field is stable on a $\gtrsim$3 yr timescale, much longer than the convective turnover time, pointing to a stable dynamo process. A recent simultaneous observation of the L dwarf binary Kelu-1 resulted in an X-ray detection without corresponding radio emission (Audard et al. 2007), although the radio limits still allow for a violation of the radio/X-ray correlation by up to $\sim 2 \times 10^3$.

Here we exploit the powerful approach of simultaneous observations to investigate the magnetic activity in the M8.5 dwarf TVLM 513−46546, an object previously detected in the radio (Berger 2002, 2006; Osten et al. 2006; Hallinan et al. 2006, 2007) and in Hα (Martin et al. 1994; Reid et al. 2002; Mohanty & Basri 2003). These observations are the first in a series that targets several objects in the sparsely studied and critical spectral type range M7–L3. In the case of TVLM 513−46546 we detect radio, X-ray, and Balmer line emission, but no UV emission. The overall behavior is complex and largely uncorrelated between the various emission bands. The long time and wavelength baselines provide unprecedented detail, including the first case to date of sinusoidal Balmer line emission; the observed 2 hr period is in excellent agreement with the rotation of TVLM 513−46546. Using the various activity indicators we infer the properties of the magnetic field, corona, and chromosphere, and show that the underlying processes and field configuration likely differ from those in early M dwarfs.

2. OBSERVATIONS

We targeted the M8.5 dwarf TVLM 513−46546 due to its vicinity ($d = 10.6$ pc; Dahn et al. 2002) and known radio and Hα activity. The bolometric luminosity of TVLM 513−46546 is $L_{\rm bol} \approx 10^{-3.59}\ L_\odot$, and its rotation velocity is $v \sin i \approx 60$ km s^{-1} (Mohanty & Basri 2003). The nondetection of lithium, with a limit of 0.05 Å, suggests that TVLM 513−46546 is most likely a very low mass star (Reid et al. 2002). Adaptive optics imaging of TVLM 513−46546 revealed no companions with $\delta m \lesssim 3$ mag in the range 0.1″–15″ (Close et al. 2003).

TVLM 513−46546 was first detected in the radio during a 2 hr observation at 8.5 GHz in 2001 September, and exhibited both persistent ($F_\nu \approx 190$ μJy) and flaring emission (Berger 2002),

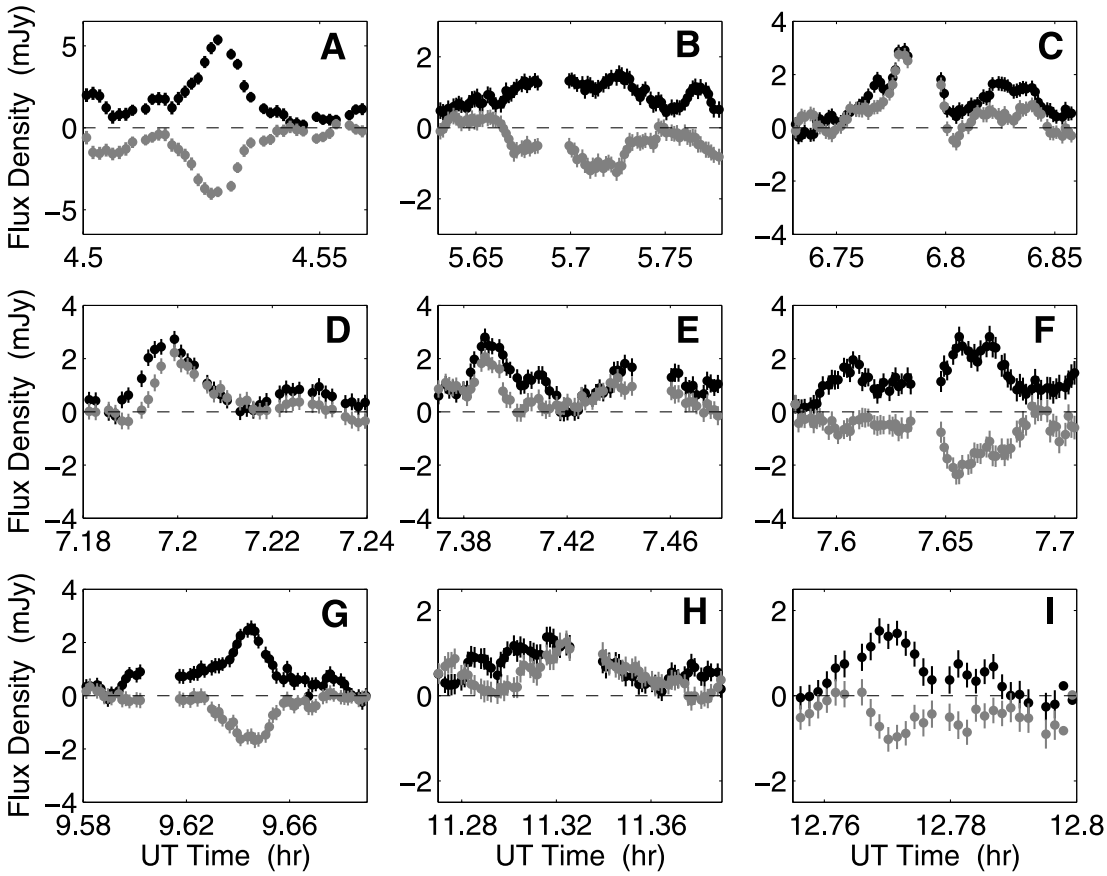

FIG. 2.—Zoom-in on individual radio flares. Total intensity (*black*) and circularly polarized flux (*gray*) are shown, smoothed with a 25 s boxcar. The error bars are 1 σ rms uncertainties. The flares exhibit diverse behavior in terms of duration, amplitude, and fraction and sense of circular polarization.

the latter with a peak brightness of 1 mJy, a duration of 15 minutes, and circular polarization of $r_c \approx 66\%$. Subsequent observations from 1.4 to 8.5 GHz in 2004 January revealed a similar level of persistent emission, $F_\nu(1.4) \approx 260$, $F_\nu(4.9) \approx 280$, and $F_\nu(8.5) \approx 230$ μJy, with $r_c \lesssim 15\%$ (Osten et al. 2006). Observations in 2005 January revealed brighter emission, $F_\nu(4.9) \approx 405$ μJy, and $F_\nu(8.5) \approx 400$ μJy, as well as a possible periodicity of about 2 hr (Hallinan et al. 2006). Finally, observations in 2006 May uncovered a series of flares with durations of a few minutes, $\sim$100% circular polarization, and a periodicity of 1.96 hr, which is also seen in *I*-band photometric monitoring (Hallinan et al. 2007; Lane et al. 2007).

Previous detections of Hα emission reveal long-term variability, with equivalent widths (EW) ranging from 1.7 to 3.5 Å, or $L_{\rm H\alpha}/L_{\rm bol} \approx 10^{-5}$ (Martin et al. 1994; Reid et al. 2002; Mohanty & Basri 2003).

Our simultaneous observations were obtained on 2007 April 20 UT for a total of 8.8 hr in the radio (04:00–12:48 UT), 8.9 hr in the X-rays (03:47–12:41 UT), and 7 hr in the optical (07:13–14:13 UT). *Swift* UV/Optical Telescope (UVOT) observations took place intermittently between 03:58 and 12:10 UT, with a total on-source exposure time of 8036 s.

2.1. *Radio*

Very Large Array[12] observations were conducted at a frequency of 8.46 GHz in the standard continuum mode with 2×50 MHz contiguous bands. Scans of 295 s on source were interleaved with 50 s scans on the phase calibrator J1513+236. The flux density scale was determined using the extragalactic source 3C 48 (J0137+331).

The data were reduced and analyzed using the Astronomical Image Processing System (AIPS). The visibility data were inspected for quality, and noisy points were removed. To search for source variability, we constructed light curves using the following method. We removed all the bright field sources using the AIPS IMAGR routine to CLEAN the region around each source, and the AIPS UVSUB routine to subtract the resulting source models from the visibility data. We then plotted the real part of the complex visibilities at the position of TVLM 513−46546 as a function of time using the AIPS DFTPL routine. The subtraction of field sources is required, since their sidelobes and the change in the shape of the synthesized beam during the observation result in flux variations over the map that may contaminate real variability or generate false variability. The resulting light curves are shown in Figures 1 and 2.

2.2. *X-Rays*

The observations were made with the *Chandra* ACIS-S3 (backside-illuminated chip), with TVLM 513−46546 offset from the on-axis focal point by 15″. A total of 29.76 ks were obtained. Data were analyzed using CIAO version 3.3, and counts were extracted in a 1″ radius circle centered on the source position. We find a total of 8 counts with energies in the range of 0.3–1.1 keV, and 2 additional counts with energies of about 10 keV (Fig. 1). Background counts were extracted from annuli centered on the source position, excluding other point sources detected in the

[12] The VLA is operated by the National Radio Astronomy Observatory, a facility of the National Science Foundation operated under cooperative agreement by Associated Universities, Inc.

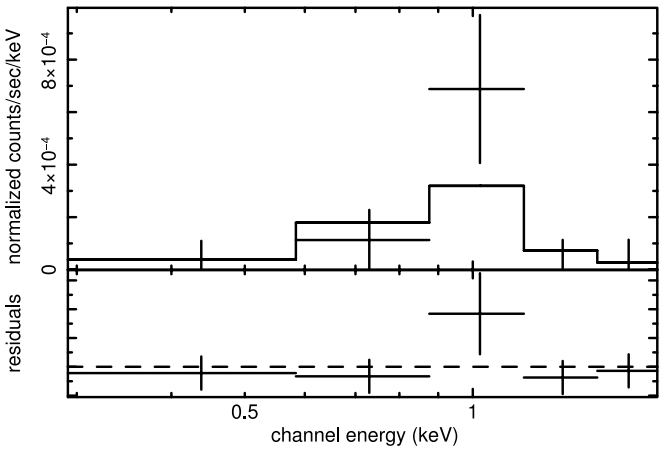

FIG. 3.—X-ray spectrum of TVLM 513−46546 in the 0.3–2 keV energy range. The best-fit Raymond-Smith model (*line*) has a temperature of about 0.9 keV.

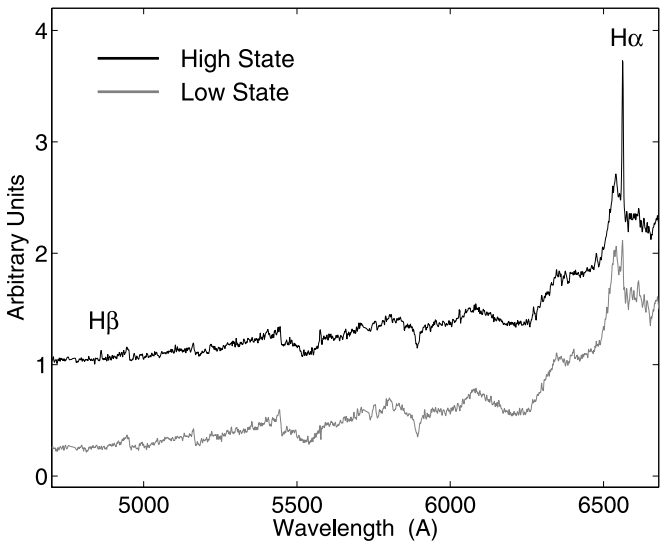

FIG. 4.—Sample optical spectra of TVLM 513−46546 in the high and low Balmer emission-line states. The high-state spectrum has been offset upward for clarity.

observation. We find that 2 background counts are expected within the source extraction aperture, likely corresponding to the two photons with ∼10 keV. Assuming Poisson statistics the number of source counts is 8^{+4}_{-3} (68% confidence), and the source count rate is therefore $2.7^{+1.3}_{-0.9} \times 10^{-4}$ s^{-1}.

To estimate the source flux and plasma temperature we fit the 0.3–2 keV spectrum using a Raymond-Smith model in `xspec11`. We find a best-fit temperature of $0.9^{+0.3}_{-0.1}$ keV, or $\approx 10^7$ K ($\chi^2_r = 0.9$ for 3 degrees of freedom; null hypothesis probability of 0.5); see Figure 3. The X-ray flux is $6.3^{+8.5}_{-2.0} \times 10^{-16}$ ergs cm^{-2} s^{-1} in the 0.3–2 keV range (1 σ including uncertainties in the count rate and model fit). At the distance of TVLM 513−46546 the corresponding luminosity is $L_X \approx 8.5^{+11}_{-3} \times 10^{24}$ ergs s^{-1}, or a ratio of $L_X/L_{bol} \approx 10^{-5.1\pm0.3}$. This detection is at the same level as the quiescent emission from the M8 dwarf VB 10 (Fleming et al. 2003), the faintest X-ray-emitting late-M dwarf to date.

We next find that of the eight detected photons four arrive as pairs with separations of 217 and 31 s (Fig. 1). The chance probabilities of such short time separations in a 29.76 ks observation are 1.7×10^{-3} and 3.4×10^{-5}, respectively. It is thus possible that the second pair constitutes a flare. Assuming the same spectral model determined above, the flare luminosity is $L_X \sim 2 \times 10^{27}$ ergs cm^{-2} s^{-1}, or $L_X/L_{bol} \sim 10^{-2.7}$, roughly similar to the saturation value found in early- and mid-M dwarfs (e.g., Fleming et al. 1993). We note that due to the small number of counts, these values are uncertain by about 0.5 dex. If the photon pair indeed represents a flare, the corresponding quiescent emission will be 25% lower than the values quoted above, or $L_X/L_{bol} \approx 10^{-5.2\pm0.3}$.

2.3. *Optical Spectroscopy*

We used[13] the Gemini Multi-Object Spectrograph (GMOS; Hook et al. 2004) mounted on the Gemini-North 8 m telescope with the B600 grating set at a central wavelength of 5250 Å, and with a 1″ slit. A series of eighty 300 s exposures were obtained with a readout time of 18 s providing 94% efficiency. The individual exposures were reduced using the `gemini` package in IRAF (for bias subtraction and flat fielding), and rectification and sky subtraction were performed using the method and software described in Kelson (2003). Wavelength calibration was performed using CuAr arc lamps, and air-to-vacuum corrections were applied. The spectrum covers 3840–6680 Å at a resolution of about 5 Å.

[13] Observations were obtained as part of program GN-2007A-Q-60.

To measure the EWs of the Hα and Hβ emission lines we use continuum regions centered on 6551 and 6572 Å, and on 4854 and 4870 Å, respectively. Sample spectra in the low and high Balmer emission state are shown in Figure 4. The Hα light curve exhibits a clear sinusoidal behavior (Fig. 1).

2.4. *Ultraviolet*

The data were obtained with the *Swift* UVOT in the UVW1 filter ($\lambda_{eff} \approx 2510$ Å), as a series of six images with exposure times ranging from 560 to 1630 s (Fig. 1). No source is detected at the position of TVLM 513−46546 in any of the individual exposures, or in the combined image with a total exposure time of 8036 s. We performed photometry on the combined exposure using a circular aperture matched to the point-spread function of the UVW1 filter (2.2″), and found a 3 σ limit of $F_\lambda(\mathrm{UVW1}) < 2.4 \times 10^{-18}$ ergs cm^{-2} s^{-1} Å^{-1}, or a Vega magnitude of $m(\mathrm{UVW1}) > 23.0$ mag. This limit corresponds to a ratio of UV to bolometric luminosity of $\lambda L_\lambda/L_{bol} < 10^{-3.2}$.

3. MULTIWAVELENGTH EMISSION PROPERTIES

We observed TVLM 513−46546 across a wide wavelength range that traces activity in various layers of the outer atmosphere. The radio emission traces particle acceleration by magnetic processes, and corresponds to gyrosynchrotron radiation or coherent radiation (electron cyclotron maser or plasma emission). The Balmer emission lines are thought to be collisionally excited in the chromosphere, and the X-ray thermal emission arises in the corona.

3.1. *Quiescent Emission*

From several flare-free regions of the radio light curve we find a quiescent flux of $F_\nu(8.5) = 208 \pm 18$ μJy, and a 3 σ limit on the fraction of circular polarization of $r_c < 25\%$. Both the flux and degree of circular polarization are similar to those measured in previous observations (§ 2), indicating that the quiescent component is stable on a multiyear timescale. Averaging of the data on timescales ranging from 1 minute to about 1 hr does not reveal any significant level of circular polarization beyond the limit quoted above.

Based on the brightness of the radio emission compared to the predicted thermal emission, and its long-term stability, we conclude that it is most likely due to gyrosynchrotron radiation. We follow

the typical assumption that the mildly relativistic electrons, which produce the radio emission, follow a power-law distribution, $N(\gamma) \propto \gamma^{-p}$ for $\gamma > \gamma_m$, with $p \sim 3$ typical for M and L dwarfs (Güdel et al. 1993b; Berger et al. 2005; Osten et al. 2006). The gyrosynchrotron emission spectrum is determined by the size of the emission region (R), the density of radiating electrons (n_e), and the magnetic field strength (B) according to (Dulk & Marsh 1982)

$$r_c = 0.3 \times 10^{1.93\cos\theta - 1.16\cos^2\theta} (3 \times 10^3/B)^{-0.21-0.37\sin\theta}, \quad (1)$$

$$\nu_m = 1.8 \times 10^4 (\sin\theta)^{0.5} (n_e R)^{0.23} B^{0.77} \text{ Hz}, \quad (2)$$

$$F_{\nu,m} = 2.5 \times 10^{-41} B^{2.48} R^3 n_e (\sin\theta)^{-1.52} \ \mu\text{Jy}, \quad (3)$$

where θ is the angle between the magnetic field and the line of sight.

From previous observations of TVLM 513−46546 it appears that the peak of the quiescent emission spectrum is $\nu_m \approx 5$ GHz (Osten et al. 2006). Using the limit $r_c < 25\%$, we infer a magnetic field strength, $B \lesssim 10$–740 G, for $\theta = 20^\circ$–80°. With this range we find $R \sim (0.8\text{–}8) \times 10^{10}$ cm, and $n_e \sim 10^2$–10^{10} cm^{-3}; the latter range is for $\theta = 80^\circ$–20°. Typical coronal densities for M dwarfs are $n_e \sim 10^{10}$–10^{13} cm^{-3} (e.g., van den Besselaar et al. 2003), suggesting that $\theta \sim 20^\circ$–30°. Thus, we find $R \sim$ few $\times$ 10^{10} cm and $B \lesssim$ few $\times 10^2$ G. We note that our results are consistent with those of Osten et al. (2006).

Finally, we turn to the observed Hα emission. The light curve exhibits clear sinusoidal behavior with a range of EWs of 1.5–5.5 Å (Fig. 1). The sinusoidal behavior indicates that the line is likely modulated by the rotation of TVLM 513−46546 rather than flares, and the emission is thus persistent in origin, at least on the timescale of our observation. Walkowicz et al. (2004) determined a multiplicative factor, $\chi \equiv f_{\lambda 6560}/f_{\rm bol}$, to convert H$\alpha$ EW to $L_{\rm H\alpha}/L_{\rm bol}$. For TVLM 513−46546, the observed $I - K = 4.3$ mag indicates $\log\chi \approx -5.3$, which matches the average value for spectral type M8.5 (Walkowicz et al. 2004). Thus, for the full range of EWs we find $\log(L_{\rm H\alpha}/L_{\rm bol}) \approx -4.6$ to -5.1. This covers the typical range of Hα emission observed from M8.5 dwarfs (West et al. 2004), as well as the range of EWs from past observations of this source (§ 2). We return to the implications of the sinusoidal variations in § 3.3.

Since the X-ray and Hα emission appear to be persistent, we can gain insight into the physical processes in the outer atmosphere by examining the energy scale in each band. In early dMe stars it has been suggested that the quiescent chromosphere may be heated by downward-directed coronal X-ray emission, with roughly half of the absorbed energy radiatively lost in the Balmer lines (Cram 1982). This is clearly not the case for TVLM 513−46546, for which we measure $L_{\rm H\alpha}/L_{\rm X} \approx 2$. This result supports more recent calculations of chromospheric heating by flaring X-ray emission that points to its negligible contribution (Allred et al. 2006).

3.2. *Radio Flares*

In addition to the persistent emission in the radio band we detect several distinct short-duration ($\delta t \sim 2$–15 minutes) flares, and a single broad brightening with a duration of about 1 hr (Figs. 1 and 2). These flares range in peak flux density from 2 to 5.5 mJy. Our observations allow the detection of flares to a 5 σ sensitivity of about 3.5 mJy in a single 5 s integration. In Figure 2 we provide a zoom-in on the most distinct flares, including both the total intensity light curve and the circular polarization light curve. About half of the flares exhibit left-circular polarization, while the other half exhibit right-circular polarization, with overall fractions of ∼50%–100%. There is no apparent regularity in the duration, brightness, arrival time, or circular polarization of the flares.

The apparently random sense of circular polarization (right- vs. left-handed) and flare arrival times suggest that the flares are produced in unrelated regions. This is contrary to the model proposed by Hallinan et al. (2007) to explain their detection of periodic flares, with $P = 1.96$ hr well matched to the rotation of TVLM 513−46546. These authors point to emission from a distinct region that is stable over at least several rotation periods. The absence of a similar behavior in our data suggests that this stability is limited to $\lesssim 1$ yr.

The variation in the sense of circular polarization from one flare to the next is also different from the uniform sense of polarization observed in radio flares from UV Cet (M5.5) and YZ CMi (M4.5). Flares in these two stars show consistent right-handed and left-handed polarization, respectively, which has been interpreted as a signature of particle acceleration in a toroidal dipole field (Kellett et al. 2002). The behavior of radio flares from TVLM 513−46546 in the current observation thus points to a multipolar field configuration.

While the quiescent radio emission is due to gyrosynchrotron radiation, the short durations and large fraction of circular polarization of the flares point to emission by coherent processes. The electron cyclotron maser (ECM) process leads to emission at the fundamental cyclotron frequency, $\nu_c = 2.8 \times 10^6 B$ Hz, while plasma radiation is dominated by the fundamental plasma frequency, $\nu_p = 9 \times 10^3 n_e^{1/2}$ Hz. In the ECM case the magnetic field strength inferred from the detection of flares at 8.46 GHz is $B \approx 3$ kG, while in the case of plasma radiation we infer an electron density of $n_e \approx 9 \times 10^{11}$ cm^{-3}. The latter should be used as an upper limit in the ECM model.

In the standard picture of the ECM (e.g., Melrose & Dulk 1982), electrons with a large pitch angle are reflected at the legs of the magnetic loop, while those with smaller angles precipitate into and heat the chromosphere. This process repeats, with the rise time of the emitted flare presumably reflecting the particle acceleration timescale. The flare decay reflects the time to precipitate out of the magnetic trap, and is thus related to the loss rate, $\tau \sim [(\Omega_L/4\pi) v/l]^{-1}$, where Ω_L is the solid angle of the loss cones, v is the electron velocity, and l is the transit length (Melrose & Dulk 1982). From our observations at 8.5 GHz we infer $v \sim c$, and hence $\tau \sim 30$ s leads to, $l \sim 10^{12}(\Omega_L/4\pi)$ cm. The actual size of the loop region is likely to be much smaller, since the accelerated electrons traverse the field lines multiple times before the maser process ceases. Thus, whereas in the case of the periodic outbursts a stable, dipolar field configuration was inferred (Hallinan et al. 2007), here it is likely that the emission is arising from a tangled, multipolar field.

Finally, the ECM processes is supposed to provide coronal and chromospheric heating as electrons precipitate out of the trap, and thus lead to increased Hα and X-ray emission. From Figure 1 it is clear that this is not the case for TVLM 513−46546. None of the radio flares are accompanied by an increase in either the Hα or X-ray emission. This may provide further support to the proposed tangled field configuration, since it will lead to chromospheric and coronal effects on a small scale that may go undetected when averaged over the stellar disk.

3.3. *Sinusoidal* Hα *Emission*

As noted above the Hα and Hβ emission lines exhibit sinusoidal variations with a periodicity of about 2 hr (Fig. 1). This

indicates that the likely origin of the Balmer line modulation is the rotation of TVLM 513−46546. Indeed with $R_* \approx 7 \times 10^9$ cm, the 2 hr period requires a rotation velocity of $v \approx 60$ km s^{-1}, in perfect agreement with the observed $v \sin i \approx 60$ km s^{-1}. If the Balmer lines are modulated by rotation, this indicates an inclination of the rotation axis relative to the line of sight of $i \approx 90^\circ$.

The likely connection to stellar rotation points to a large-scale ($f \sim 50\%$) hot spot located on one hemisphere of TVLM 513−46546, or an emission "bubble" that may extend to several times the stellar radius, and is occulted by the star for about half a rotation period. The fact that the Balmer lines do not completely disappear during the light-curve minima suggests that in both scenarios the solid angle subtended by the emission region is larger than the stellar disk, or alternatively, that the minima represent the baseline chromospheric emission, while the rotation of an extended bubble or a hot spot into our line of sight produces the maxima.

It also appears from the Hα light curve that the peak EW decreases with time (Fig. 1). The first peak has EW ≈ 5.5 Å followed by about 4.5 Å for the two subsequent peaks, and about 3.8 Å for the fourth peak. While our observations start during the decline of a preceding cycle, an extrapolation back to the time of the expected peak indicates an EW of at least 6 Å. The EWs at the minima, however, appear to be more stable, with perhaps a slight decrease from 2 to 1.5 Å during our observation. These trends suggest that the hot spot or extended bubble may be transitory, possibly excited by an energetic event prior to the beginning of our observations. Extrapolating the observed trend, we find that the peak Hα EW will match the baseline level of 1.5 Å about 7 hr after the end of our observation. Future observations of TVLM 513−46546 are crucial for assessing whether this is in fact a transient feature.

We further find no clear correspondence between the peaks of Hα emission and the radio flares. In fact, the opposite may be the case. The three Hα minima that have simultaneous radio coverage appear to roughly coincide with radio flares. If we extrapolate the Hα light curve back in time, we find that a previous minimum also appears to coincide with a radio flare (at about 05:40 UT). However, other radio flares, including the brightest one detected, do not coincide with observed or extrapolated Hα minima, suggesting that this anticorrelation between Hα and radio emission may be a result of small-number statistics.

The detection of a 2 hr period in two different emission bands and at two different times with no clear correspondence indicates that the radio flares are not sufficiently energetic, or impact a large enough scale to influence the chromosphere. This behavior also suggests that the magnetic field configuration of TVLM 513−46546 may be composed of a large-scale dipolar field, as well as a more compact and tangled component, which give rise to periodic signals at different times and wave bands.

4. LACK OF RADIO/X-RAY CORRELATION

TVLM 513−46546 is only the third ultracool dwarf to be observed simultaneously in the radio and X-rays, allowing a continued investigation of the radio/X-ray correlation in these objects. Coronally active stars up to spectral type M7, including the Sun, exhibit a tight correlation between their radio and X-ray emission (Güdel & Benz 1993; Benz & Güdel 1994). The persistent emission follows a linear trend, $L_R \approx 3 \times 10^{-16}\ L_X$ Hz^{-1}, which extends over 6 orders of magnitude in L_R (Güdel & Benz 1993), while for flares the relation is $L_R \approx 5.4 \times 10^{-27}\ L_X^{1.37}$ Hz^{-1} over 8 orders of magnitude in L_R (Benz & Güdel 1994); see Figure 5.

From several previous (nonsimultaneous) observations it has become clear that the above correlations break down in at least some ultracool dwarfs (Berger et al. 2001, 2005; Berger 2002, 2006), with a clear transition occurring at spectral type M7 (Berger 2006). This conclusion was supported by our simultaneous observations of the L3.5 dwarf 2MASS J00361617+1821104 (Berger et al. 2005). Here we find continued evidence for this trend. Using the persistent radio and X-ray luminosities we find $L_R/L_X \approx 3.3 \times 10^{-12}$ Hz^{-1}, a factor of 10^4 times larger than expected. This is similar to the level of excess radio emission observed in the previous late-M and L dwarfs. If we take into account the flaring emission, with a typical peak luminosity of $L_R \approx 4 \times 10^{14}$ ergs cm^{-2} s^{-1} Hz^{-1}, and assume that the single X-ray photon pair with $L_X \approx 2 \times 10^{27}$ ergs cm^{-2} s^{-1} is indeed a flare (§ 2.2), we find that for flares $L_R/L_X \approx 2 \times 10^{-13}$ Hz^{-1}, a factor of about 3×10^3 larger than expected.

The radio/X-ray correlation has been interpreted in the context of the Neupert effect (Neupert 1968). In this scenario, the radio emission is produced when coronal magnetic loops reconnect and create a current sheet along which ambient electrons are accelerated. The accelerated electrons in turn drive an outflow of hot plasma into the corona as they interact with and evaporate the underlying chromospheric material. The interaction of the outflowing plasma with the electrons produces X-ray emission via the bremsstrahlung process. This mechanism points to a causal connection between particle acceleration, which is the source of radio emission, and plasma heating, which results in X-ray emission. Thus, the X-ray thermal energy should simply be related by a constant of proportionality to the integrated radio flux. The breakdown in the radio/X-ray correlation, and the clear lack of correspondence between the radio flares observed on TVLM 513−46546 and its X-ray emission suggest that the heating of coronal material is generally inefficient in objects later than M7. This may be due to the short lifetime and small size of the flare-emitting regions (i.e., in the case that they arise from highly tangled and multipolar fields), or to lower efficiency of coronal heating so that the bulk of the coronal emission is at temperatures lower than $kT \sim 1$ keV.

5. DISCUSSION AND CONCLUSIONS

We presented simultaneous radio, X-ray, UV, and optical spectroscopic observations of the M8.5 dwarf TVLM 513−46546 that probe magnetic activity and its influence on the stellar chromosphere and corona. These observations are the first in a series of several objects that span the sparsely studied spectral type range M7–L3, over which the magnetic activity appears to exhibit a change in behavior compared to early spectral types. We find that TVLM 513−46546 exhibits a wide range of both quiescent and flaring activity that includes radio emission from large- and small-scale regions, coronal soft X-ray emission, and sinusoidal and periodic Balmer line emission from a chromospheric hot spot or an extended structure with a covering fraction of about 50%.

Quantitatively, we find that the quiescent radio emission is produced on the scale of the entire stellar disk, with a magnetic field of $\sim 10^2$ G. From portions of the light curve that are free of flares we see no evidence for variability of this persistent component. Moreover, the similarity in flux level to observations carried over the past 6 years indicates that the magnetic field is stable on timescales significantly longer than the convective turnover time, $\tau_{\rm conv} \sim 10^2$ days (Chabrier & Baraffe 2000). This is similar to the situation we observed in 2MASS J00361617+1821104 (L3.5), with a periodic radio signal that was stable over at least 3 years (Berger et al. 2005).

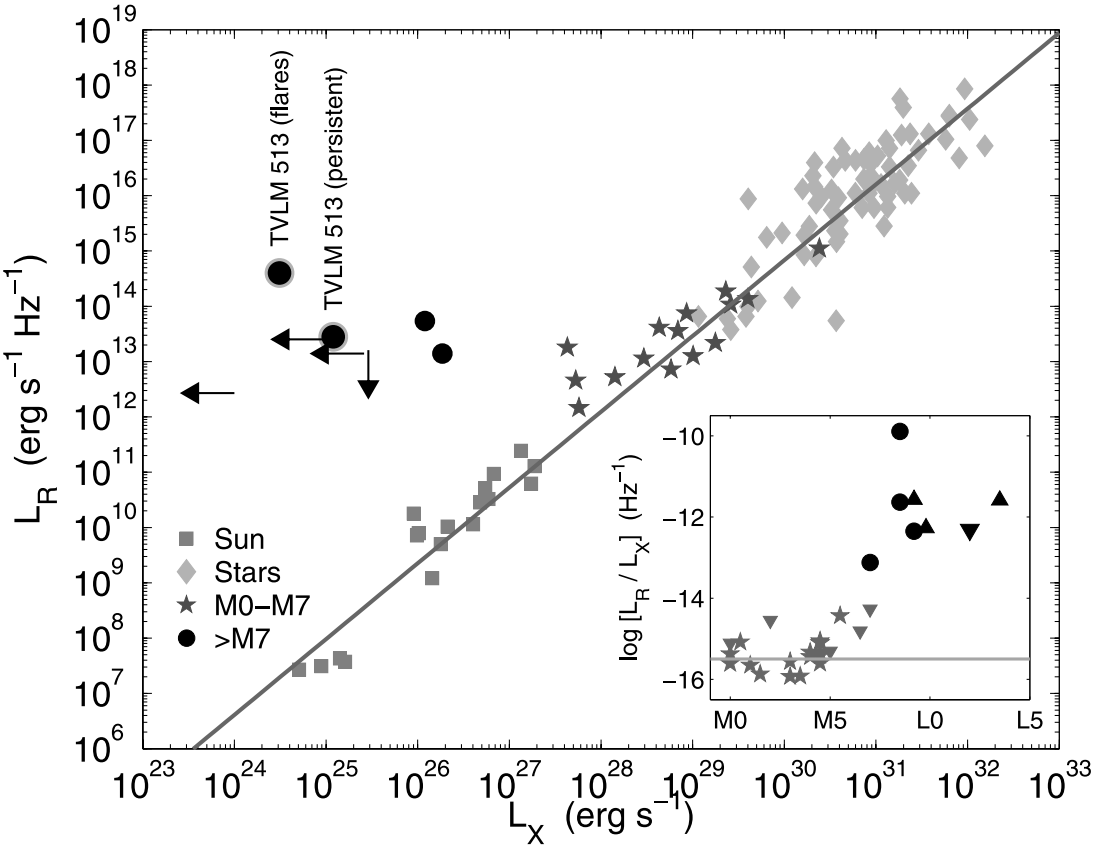

FIG. 5.—Radio vs. X-ray luminosity for stars exhibiting coronal activity. Data for late-M and L dwarfs are from Rutledge et al. (2000), Berger et al. (2001, 2005), Berger (2002, 2006), Burgasser & Putman (2005), and Audard et al. (2007), while other data are taken from Güdel (2002) and references therein. Data for the Sun include impulsive and gradual flares, as well as microflares. The strong correlation between L_R and L_X is evident, but it begins to break down around spectral type M7 (see inset).

We also find from a comparison of the radio and X-ray data that the magnetic field axis is likely highly inclined relative to the rotation axis of TVLM 513−46546, which is inferred from the 2 hr period of the Hα emission to be about 90° (§ 3.3). This is an interesting result in the context of magnetic dynamo models of fully convective stars. Chabrier & Küker (2006) and Dobler et al. (2006) found that the α^2 dynamo, which relies on a stratified and rotating turbulent medium, leads to a nonaxisymmetric field with an overall configuration that lies in the equatorial plane. This seems to be supported by our observations.

The X-ray emission requires coronal plasma with $T \approx 10^7$ K, similar to those of early M dwarfs. The energy input from the X-ray-emitting corona is similar to, or somewhat smaller than, the radiative losses in the Balmer emission lines, indicating that the chromosphere is at least partly heated by the overlying corona. It is possible, however, that the somewhat elevated chromospheric luminosity is the result of an energy input process that took place before the start of our observations. This latter possibility is supported by the apparently decreasing level of peak Hα flux during our observation, and the nearly constant baseline level traced by the light-curve minima. Indeed, the Hα luminosity during the minima is about half of the X-ray luminosity.

In addition to the persistent emission, we detect a large number of radio flares with a range of peak fluxes, durations, and degrees of circular polarization. The overall short durations of the flares and large degree of circular polarization are indicative of coherent emission. In the context of the ECM mechanism, the inferred magnetic field is about 3 kG, similar to fields on the most active early M dwarfs (Saar & Linsky 1985; Johns-Krull & Valenti 1996). Similar flares have been detected in previous observations of TVLM 513−46546, but with a 2 hr periodicity that is absent in our data. The 2 hr period was attributed to compact polar regions in a dipolar field rotating in and out of our line of sight (Hallinan et al. 2007). The durations of the flares detected here, and their random arrival times and sense of circular polarization, point instead to a tangled and multipolar field. Thus, the conditions required for coronal coherent radio flares exist on long timescales, but the change in behavior may signal a shift in the field configuration on $\lesssim$1 yr timescales. The inferred multipolar nature of the field is again in good agreement with models of the α^2 dynamo, which suggest that the bulk of the energy is in the quadrupolar and higher order components.

Unlike in the radio flares, we do find clear Hα periodicity ($P \approx 2$ hr), with a sinusoidal light curve that reveals the presence of a chromospheric hot spot, or an extended bubble, with a covering fraction of about 50%. It is unclear whether this emission region is stable over timescales longer than about 1 day, but the decrease in peak flux between subsequent rotations may point to a transient nature that may be similar to the one now inferred in the radio band. The observed 2 hr period is well matched to the measured rotation velocity of TVLM 513−46546, and indicates a rotation axis inclination of about 90° (see also Hallinan et al. 2007; Lane et al. 2007). The existence of such an extended structure provides additional support for a large-scale field that dominates the quiescent radio and X-ray emission.

The general wisdom in the study of magnetic activity and its impact on the outer atmosphere is that the input of magnetic energy results in a series of related events that heat the corona and chromosphere and result in correlated X-ray, radio, and optical line emission. This idea is supported by observations of the Sun,

as well as various samples of early M dwarfs. The observations presented here show no clear evidence for any correlation between the various activity bands. In particular, the quiescent radio emission is overluminous by nearly 4 orders of magnitude compared to predictions from the radio/X-ray correlation. Similarly, the radio flares do not appear to correlate with the Hα variability. Finally, it is possible that the X-ray flux incident on the chromosphere is not sufficient to produce the observed Hα luminosity (particularly if we include the contribution from higher order Balmer lines).

Taking these various observations and inferences into account we therefore conclude that the observations of TVLM 513−46546 indicate the following:

1. Ultracool dwarfs exhibit clear evidence for intense magnetic activity that is not diminished compared to early M dwarfs. This activity is manifested most clearly in the centimeter radio band, but also in X-rays and Balmer line emission.
2. Both a chromosphere and a corona exist, with luminosities relative to the bolometric luminosity that are in line with other objects of similar spectral type, and are significantly lower (by $\sim$2 orders of magnitude) compared to early M dwarfs.
3. The dissipation of magnetic energy in the form of intense radio flares does not have a clear effect on chromospheric and coronal emission, both temporally and in terms of overall luminosity. The radio/X-ray correlation is violated by about 4 orders of magnitude both in quiescence and during flares.
4. The presence of a steady large-scale magnetic field, as well as a multipolar component, supports current models of α^2 dynamos in fully convective stars.

Simultaneous multiwavelength observations of several additional ultracool dwarfs are in progress. We expect that with this larger sample, and with the longer time baselines of our observations compared to typical studies, we can begin to address in detail the range of quiescent and variable activity, and the absence or presence of the correlations that appear to exist in the early M dwarfs. Ultimately, these observations should reveal the energy and size scale of the magnetic field, and thus provide a detailed view of the magnetic generation process in fully convective stars.

We thank the *Chandra*, Gemini, VLA, and *Swift* schedulers for their invaluable help in coordinating these observations. This work has made use of the SIMBAD database, operated at CDS, Strasbourg, France. Based in part on observations obtained at the Gemini Observatory, which is operated by the Association of Universities for Research in Astronomy, Inc., under a cooperative agreement with the NSF on behalf of the Gemini partnership: the National Science Foundation (United States), the Science and Technology Facilities Council (United Kingdom), the National Research Council (Canada), CONICYT (Chile), the Australian Research Council (Australia), CNPq (Brazil), and CONICET (Argentina). Data from the UVOT instrument on *Swift* were used in this work. *Swift* is an international observatory developed and operated in the US, UK, and Italy, and managed by the NASA Goddard Space Flight Center with operations center at Penn State University. Support for this work was provided by the National Aeronautics and Space Administration through *Chandra* Award Number G07-8014A issued by the *Chandra* X-Ray Observatory Center, which is operated by the Smithsonian Astrophysical Observatory for and on behalf of the National Aeronautics Space Administration under contract NAS8-03060. E. B. is supported by NASA through Hubble Fellowship grant HST-01171.01 awarded by the STScI, which is operated by AURA, Inc., for NASA under contract NAS 5-26555.

REFERENCES

Allred, J. C., Hawley, S. L., Abbett, W. P., & Carlsson, M. 2006, ApJ, 644, 484
Antonova, A., Doyle, J. G., Hallinan, G., Golden, A., & Koen, C. 2007, A&A, 472, 257
Audard, M., Osten, R. A., Brown, A., Briggs, K. R., Güdel, M., Hodges-Kluck, E., & Gizis, J. E. 2007, A&A, 471, L63
Basri, G., & Marcy, G. W. 1995, AJ, 109, 762
Benz, A. O., & Güdel, M. 1994, A&A, 285, 621
Berger, E. 2002, ApJ, 572, 503
———. 2006, ApJ, 648, 629
Berger, E., et al. 2001, Nature, 410, 338
———. 2005, ApJ, 627, 960
Burgasser, A. J., & Putman, M. E. 2005, ApJ, 626, 486
Chabrier, G., & Baraffe, I. 2000, ARA&A, 38, 337
Chabrier, G., & Küker, M. 2006, A&A, 446, 1027
Close, L. M., Siegler, N., Freed, M., & Biller, B. 2003, ApJ, 587, 407
Cram, L. E. 1982, ApJ, 253, 768
Dahn, C. C., et al. 2002, AJ, 124, 1170
Dobler, W., Stix, M., & Brandenburg, A. 2006, ApJ, 638, 336
Dulk, G. A., & Marsh, K. A. 1982, ApJ, 259, 350
Fleming, T. A., Giampapa, M. S., & Garza, D. 2003, ApJ, 594, 982
Fleming, T. A., Giampapa, M. S., Schmitt, J. H. M. M., & Bookbinder, J. A. 1993, ApJ, 410, 387
Gizis, J. E., Monet, D. G., Reid, I. N., Kirkpatrick, J. D., Liebert, J., & Williams, R. J. 2000, AJ, 120, 1085
Güdel, M. 2002, ARA&A, 40, 217
Güdel, M., & Benz, A. O. 1993, ApJ, 405, L63
Güdel, M., Benz, A. O., Schmitt, J. H. M. M., & Skinner, S. L. 1996, ApJ, 471, 1002
Güdel, M., Schmitt, J. H. M. M., Bookbinder, J. A., & Fleming, T. A. 1993a, ApJ, 415, 236
———. 1993b, ApJ, 415, 236
Hallinan, G., Antonova, A., Doyle, J. G., Bourke, S., Brisken, W. F., & Golden, A. 2006, ApJ, 653, 690
Hallinan, G., et al. 2007, ApJ, 663, L25
Hawley, S. L., et al. 1995, ApJ, 453, 464
Hook, I. M., Jørgensen, I., Allington-Smith, J. R., Davies, R. L., Metcalfe, N., Murowinski, R. G., & Crampton, D. 2004, PASP, 116, 425
Johns-Krull, C. M., & Valenti, J. A. 1996, ApJ, 459, L95
Kellett, B. J., Bingham, R., Cairns, R. A., & Tsikoudi, V. 2002, MNRAS, 329, 102
Kelson, D. D. 2003, PASP, 115, 688
Lane, C., et al. 2007, ApJ, 668, L163
Liebert, J., Kirkpatrick, J. D., Cruz, K. L., Reid, I. N., Burgasser, A., Tinney, C. G., & Gizis, J. E. 2003, AJ, 125, 343
Martin, E. L., Rebolo, R., & Magazzu, A. 1994, ApJ, 436, 262
Melrose, D. B., & Dulk, G. A. 1982, ApJ, 259, 844
Mohanty, S., & Basri, G. 2003, ApJ, 583, 451
Mohanty, S., Basri, G., Shu, F., Allard, F., & Chabrier, G. 2002, ApJ, 571, 469
Neupert, W. M. 1968, ApJ, 153, L59
Osten, R. A., Hawley, S. L., Bastian, T. S., & Reid, I. N. 2006, ApJ, 637, 518
Pallavicini, R., Golub, L., Rosner, R., Vaiana, G. S., Ayres, T., & Linsky, J. L. 1981, ApJ, 248, 279
Phan-Bao, N., Osten, R. A., Lim, J., Martín, E. L., & Ho, P. T. P. 2007, ApJ, 658, 553
Pizzolato, N., Maggio, A., Micela, G., Sciortino, S., & Ventura, P. 2003, A&A, 397, 147
Reid, I. N., Kirkpatrick, J. D., Gizis, J. E., & Liebert, J. 1999, ApJ, 527, L105
Reid, I. N., Kirkpatrick, J. D., Liebert, J., Gizis, J. E., Dahn, C. C., & Monet, D. G. 2002, AJ, 124, 519
Rosner, R., Golub, L., & Vaiana, G. S. 1985, ARA&A, 23, 413
Rutledge, R. E., Basri, G., Martín, E. L., & Bildsten, L. 2000, ApJ, 538, L141
Saar, S. H., & Linsky, J. L. 1985, ApJ, 299, L47
van den Besselaar, E. J. M., Raassen, A. J. J., Mewe, R., van der Meer, R. L. J., Güdel, M., & Audard, M. 2003, A&A, 411, 587
Vilhu, O., & Walter, F. M. 1987, ApJ, 321, 958
Walkowicz, L. M., Hawley, S. L., & West, A. A. 2004, PASP, 116, 1105
West, A. A., et al. 2004, AJ, 128, 426